Inclusive Production of the $\rho^{\pm}(770)$ Meson in Hadronic Decays of the Z^0 Boson

Ph.D. Thesis
in
Engineering Physics
University of Gaziantep

Supervisor: ***Assoc. Prof. Dr. Ayda BEDDALL***
Co-supervisor: ***Assist. Prof. Dr. Andrew BEDDALL***

By
Ahmet BİNGÜL
April 2007

Introduction

High energy collisions of sub-atomic particles can result in events containing a high multiplicity of hadronic particles.

An example was the production of Z^0 Bosons at LEP an e^+e^- collider with E_{CM} = 91.2 GeV (≈ 1.5 x 10^{-8} Joules)

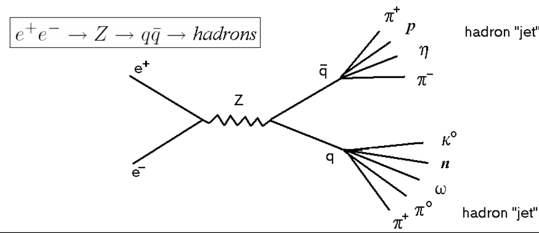

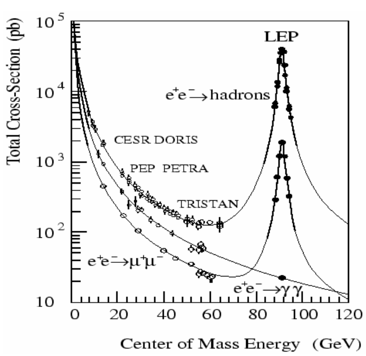

The Standard Model

Table 2.1: *The particles and forces of the Standard Model.*

Fermions (spin − ½)				Bosons (spin 1)		
Quarks		Leptons		em.	Weak	Strong
u (up)	d (down)	e^-	ν_e			
c (charm)	s (strange)	μ^-	ν_μ	γ	$W^{\pm}$, Z	gluons(8)
t (top)	b (bottom)	τ^-	ν_τ			

The transition:

quarks and gluons → hadrons

can only be described by *phenomenological models*.

The measurement of inclusive particle production cross sections of *resonant states* (e.g: ***ω*** or ***ρ***) improves the description of the *hadronization process.*

LEP was ideal for studying hadronization.

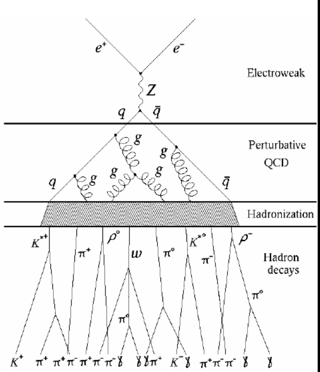

This study describes the **ALEPH** measurement of

- the production rate and
- the differential cross section

of the $\rho^{\pm}(770)$ meson in hadronic decays of the Z boson.

$\rho^{\pm}$ candidates are reconstructed from the decay channel:

$$\rho^{\pm} \to \pi^0 + \pi^{\pm} \quad (BR \approx 100\%)$$

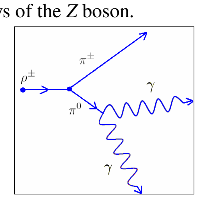

The results are compared with:

- **JETSET 7.4** (a Monte Carlo event generator software)
- **OPAL** measurement (unique at LEP)

The Large Electron-Positron Collider (LEP)

- Circumference 27 km (largest e^+e^- collider)
- Located in an underground at a depth about 100 m
- Operated
  between 1989 – 1995; E_{CM} = 91.2 GeV for **Z**
  between 1995 – 2000; E_{CM} = 160–190 GeV for **W⁺W⁻**
  for
  ALEPH,
  DELPHI,
  OPAL and L3
  experiments

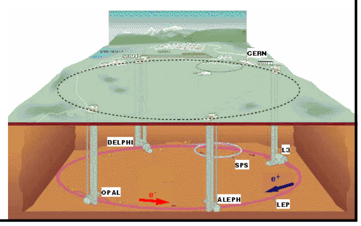

Particle Detectors

Detectors employed in HEP experiments record
position, *arrival time*, *momentum*, *energy* and *identity*
of particles.

Charged particles ($e^\pm$ p $K^\pm$ $\mu^\pm$ $\pi^\pm$)
can be detected through their ionisation in tracking chambers

* a measure of the curvature of the track in a magnetic field gives a measure of its momentum

* a measure of the rate of ionisation loss (dE/dx) can be used to determine its type

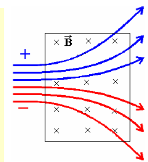

Neutral particles (γ n)
are detected via calorimeters, where their position and energy are measured.

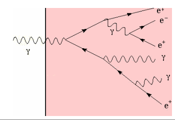

Different particle types interact differently with matter
e.g. photons do not feel a magnetic field

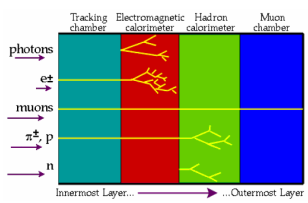

We need different types of detectectors
to measure different types of particles.

The ALEPH Detector

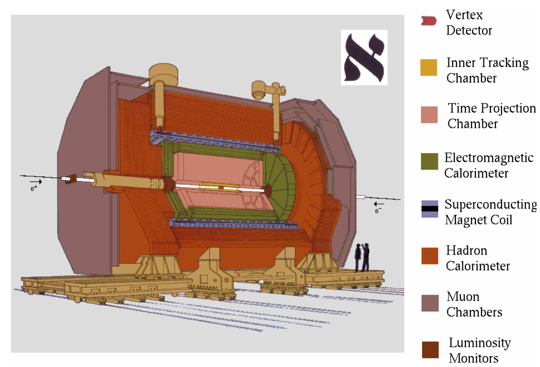

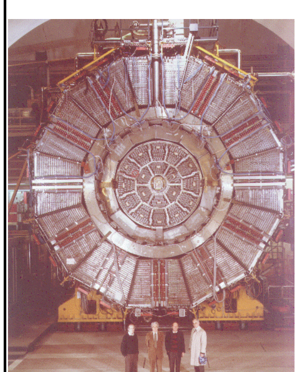

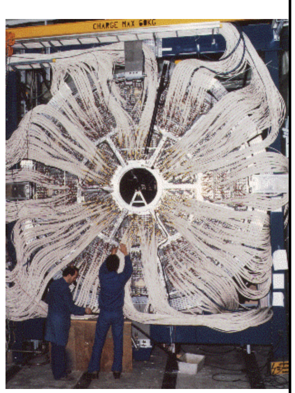

Tracking Chambers

Detector	Resolution	Photo
Vertex Detector (**VDET**)	$\sigma(r,\phi) = 12\ \mu\text{m}$ $\sigma(z) = 10\ \mu\text{m}$	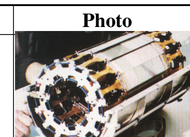
Inner Tracking Chamber (**ITC**)	$\sigma(r,\phi) = 20\ \mu\text{m}$	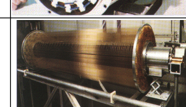
Time Projection Chamber (**TPC**)	$\sigma(r,\phi) = 180\ \mu\text{m}$ $\sigma(z) = 1\ \text{mm}$ $\sigma(p) = 1.2 \times 10^{-3} p^2\ \text{GeV/c}$	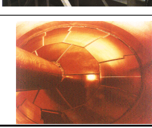

Electromagnetic Calorimeter (ECAL)

For electrons and photons of high energy, a dramatic result of the combined phenomena of bramsstrahlung and pair production is the occurance of cascade showers.

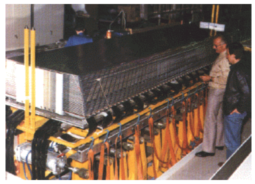

A parent electron will radiate photons, which converts to pairs, which radiate and produce fresh pairs in turn, the number of particles increasing exponentially with depth in the medium.

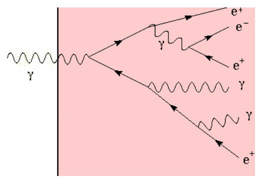

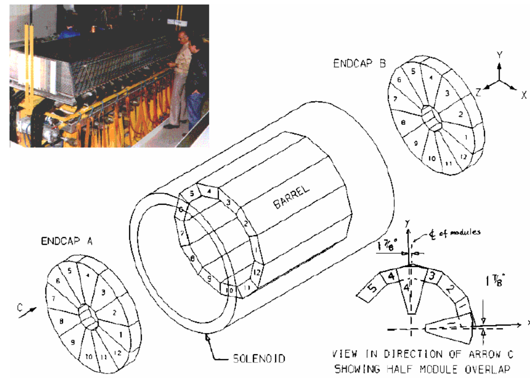

Energy resolution

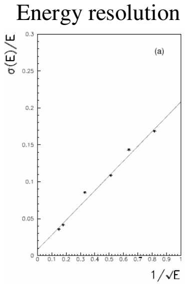

Spatial resolution

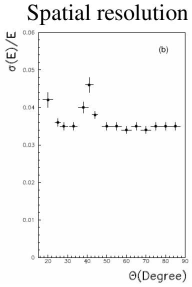

$$\frac{\sigma_E}{E} = \frac{0.18}{\sqrt{E}} + 0.009$$

$$\sigma_{\theta,\phi} = \left(\frac{2.5}{\sqrt{E}} + 0.25\right) \text{ mrad}$$

Event Reconstruction and Simulation

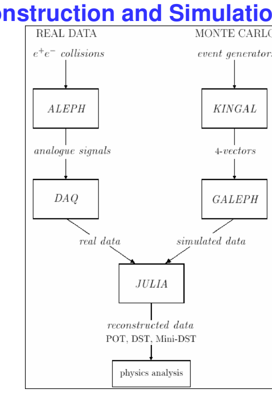

Event Selection

The ALEPH detector recorded a variety of events

- $\gamma\gamma$ events
- most of decays of Z boson to its various modes

Z Decay Mode	Fraction (%)
$Z \to e^+e^-$	3.363 ± 0.004
$Z \to \mu^+\mu^-$	3.366 ± 0.007
$Z \to \tau^+\tau^-$	3.370 ± 0.008
$Z \to q\bar{q}$ **hadrons**	69.910 ± 0.060
$Z \to \nu\bar{\nu}$ **invisible**	20.000 ± 0.060

In addition, there are small number of background:
– beam-gas interaction
– beam electrons
– cosmic rays

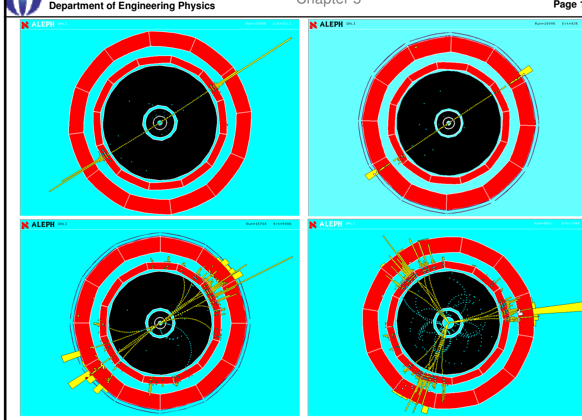

To remove events which suffer from a low geometric acceptance, a cut applied on the polar angle, θ, of the event axis as defined by sphericity.

Events are accepted if
$35^{o} < \theta < 145^{o}$
($|\cos\theta|<0.82$)

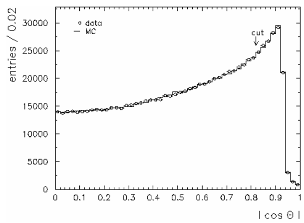

Hadronic Event Selection

Hadronic events are selected on the basis of the total charged multiplicity and energy within an event.
For this, cuts are applied to select 'good charged tracks'.

Track Cuts
removes same badly reconstructed tracks.

A good charged track must have:

- at least 4 TPC hits
- a polar angle $20^{o} < \theta < 160^{o}$
- a transverse impact parameter $|d_0|<2$ cm
- a longitudinal impact parameter $|z_0|< 5$cm
- a transverse momentum $p_t > 200$ MeV/c

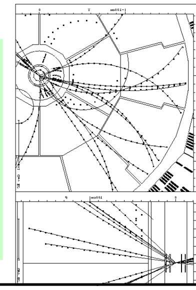

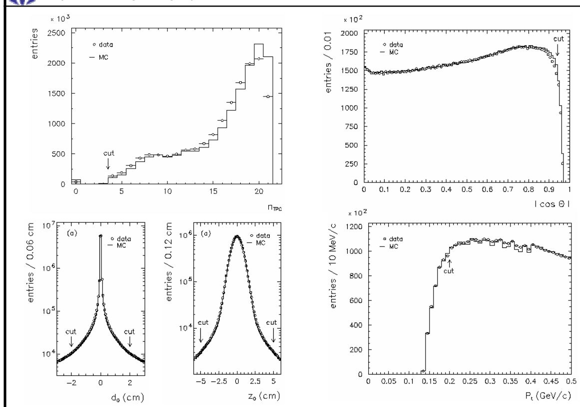

Event Cuts

1. a minimum of 5 'good' tracks
2. a minimum of 15 GeV total 'good' charged energy

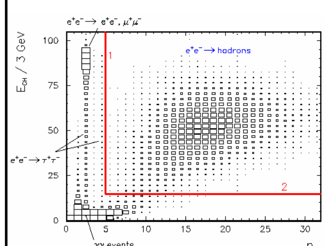

With these cuts a total

3,239,746 hadronic events

are selected with

efficiency: $\varepsilon = 95.0$ %
purity : $P = 99.6$ %

from data recorded by ALEPH from 1991 to 1995 running periods.

Flow chart of hadronic event selection:

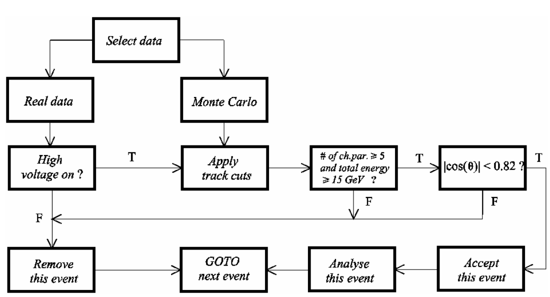

Track Selection

$\rho^{\pm}$ candidates are reconstructed from the decay channel:

$$\rho^{\pm} \rightarrow \pi^{0} + \pi^{\pm} \quad (BR \approx 100\%)$$

$\pi^{\pm}$ selection is relatively trivial, while
π^{0} selection and reconstruction is more complicated.

All selection performances are determined from the Monte Carlo with the aim to maximise both purity and efficiency.

Charged Track Selection

All good tracks originating from IP are considered as pions.

The following cuts select $\pi^{\pm}$ with
$\varepsilon = 95\%$ and $P = 43\%$

- a transverse impact parameter $|d_0|<0.5$ cm
- longitudinal impact parameter $|z_0|< 3.0$ cm
- a transverse momentum $p_t > 250$ MeV/c
- if available, $-2 < \chi(dE/dx) < 3$ (with pion hypothesis)

Tight cuts on the impact parameters are introduced to increase the reconstruction purity of $\pi^{\pm}$ mesons from $\rho^{\pm}$.

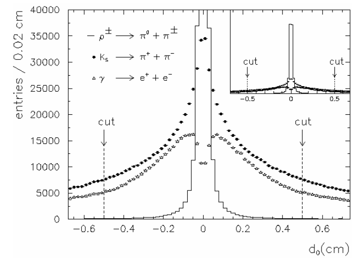

Charged particle identification is performed by the measurement of ionisation energy loss, **dE/dx**.

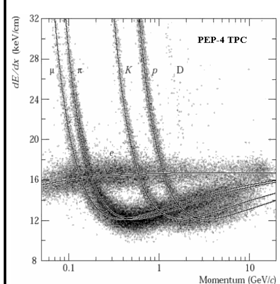

The deviation from an assumed hypothesis expressed as:

$$\chi(\mathrm{dE/dx}) = \frac{(\frac{\mathrm{dE}}{\mathrm{dx}})_{\mathrm{measured}} - (\frac{\mathrm{dE}}{\mathrm{dx}})_{\mathrm{expected}}}{\sigma_{\mathrm{dE/dx}}}$$

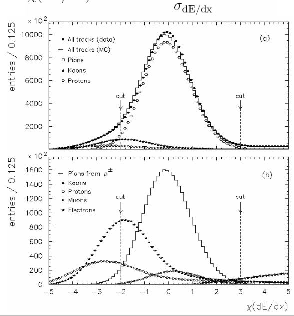

Neutral Pion Selection

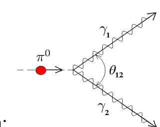

Neutral pions are built from the decay

$$\pi^0 \longrightarrow \gamma + \gamma$$

Invariant mass spectra is built up by the equation:

$$M^2 = 2E_1E_2(1 - \cos\theta_{12})$$

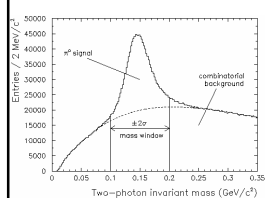

***Following cuts are applied*:**

- Each photon energy $E\gamma > 1$ GeV
- Pion energy $E\pi < 18$ GeV
- Invariant mass of two photon $M(\gamma_1,\gamma_2)$, should be within $\pm 2\sigma$ mass window around pion signal.
  σ is defined as HWHM.

Poor purity of the pions are improved by a **'Ranking' Method.**

The **topology** of reconstructed π^0 is found to be important.

Geometric representation of four possible π^0 topologies are given right.

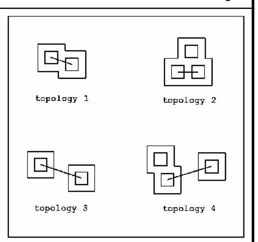

Photon pairs taken from:
topology 1: one ECAL cluster, within which two subclusters are resolved
topology 2: one ECAL cluster, within which more than two subclusters are resolved
topology 3: two ECAL clusters, within each of which no subclusters are resolved
topology 4: two ECAL clusters, within one or both of which more than one subcluster is resolved

Mass Constraint

Uncertainties in the reconstructed momentum vector of a π^0 are introduced due to the finite ECAL spatial and energy resolution.

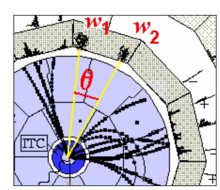

To improve the momentum resolution of the pion the reconstructed mass can be constrained to the nominal pion mass of 135 MeV/c².
This is done by modifying the photon energies (E_1 and E_2) and opening angle (θ) between photons until the required mass is obtained. These parameters can be found by minimising the chi-square form:

$$\chi^2 = (\frac{E_1 - \omega_1}{\sigma_1})^2 + (\frac{E_2 - \omega_2}{\sigma_2})^2 + (\frac{\cos\theta_{\gamma\gamma} - K}{\sigma_{\cos\theta_{\gamma\gamma}}})^2$$

with mass constraint:

$$M_{\pi^0}^2 = 2E_1E_2(1 - K)$$

Neutral Pion Calibration

Selecting π^0 candidates from a mass window around the π^0 peak provides initial rejection of most of the combinatorial background.

It is found that: peak mass and width of the π^0 signal depend on both energy and topology.

So, we need to calibrate two functions

$$m(E,T) \text{ and } \sigma(E,T)$$

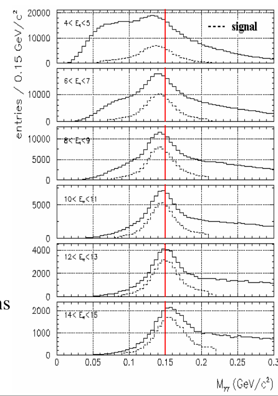

The calibration procedure is as follows:

1. The mass spectra is plotted for the matched pion signal (for each topology in 1 GeV energy intervals)
2. The peak (signal) is fitted with a Gaussian from which positions *a* and *b*, taken at half height, are measured
3. Half width at half maximum HWHM $\sigma = (b-a)/2$ and the center of the mass window $m = (b+a)/2$ are evaluated

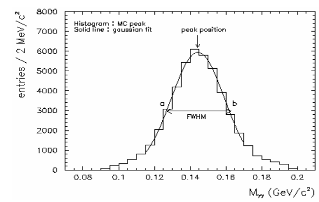

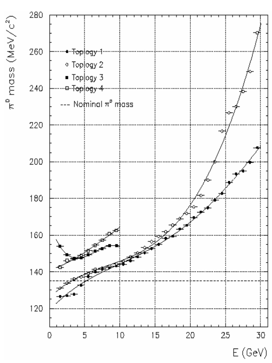

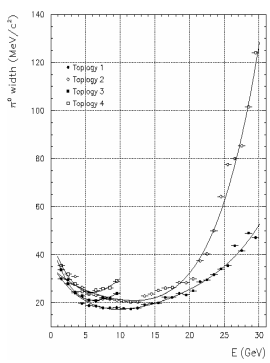

An example to show the performance of the calibration for each topology for pion energy between

$2\ GeV < E_{\pi^0} < 3\ GeV$

The calibration functions give a correct selection of π^0 peak.

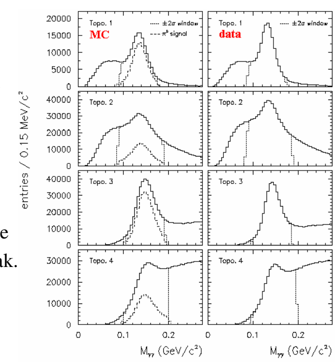

The Ranking Method

Consider **n** photons taken from the ECAL. We can form π^0 candidates by building photon pairs as follows:

PHOTONS	SELECTED PAIRS (combinations)
1	12 23 34 45 ... (n-1)n
2	13 24 35 . .
3	14 25 . . .
4	15 . . .
5	. . . 4n
.	. . 3n
.	. 2n
n	1n

Number of combinations:

$$C(n,2) = \frac{n!}{2!(n-2)!} = \frac{n(n-1)}{2}$$

we have $n(n-1)/2$ candidates forming *S+B* but only $n/2$ of them are true forming *S*.

Signal-to-background ratio:

$$\frac{S}{B} = \frac{n/2}{n(n-1)/2 - n/2} = \frac{1}{n-2}$$

Purity and Efficiency

In this study, we define the neutral pion purity ($\mathcal{P}$) and efficiency (ε) as follows:

$$\mathcal{P} = \frac{S}{S+B} \qquad \varepsilon = \frac{S}{S_0}$$

$$\varepsilon \times \mathcal{P} = \frac{1}{S_0}\left(\frac{S}{\sqrt{S+B}}\right)^2$$

$$\frac{S}{\sqrt{S+B}} \longrightarrow$$ **signal significance**

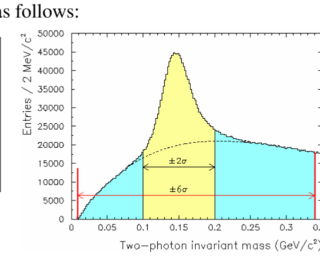

where:
S is the number of signal, and
B is the number of background for the given mass window and
S_0 is the total number of signal within $\pm 6\sigma$ mass window

The Standard Method

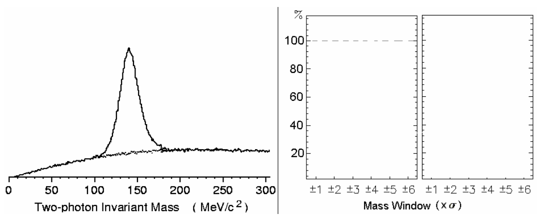

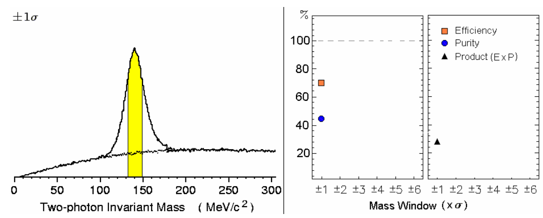

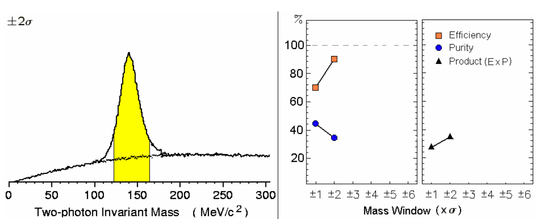

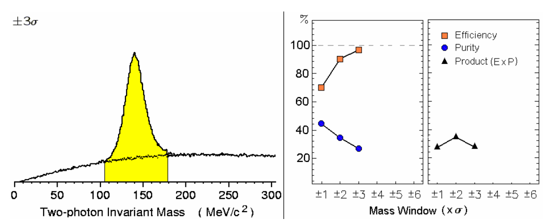

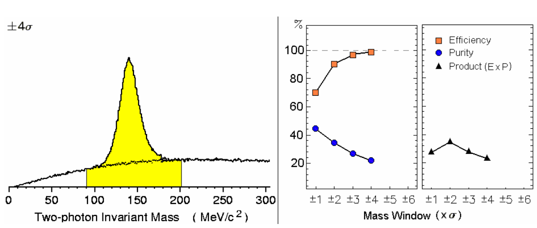

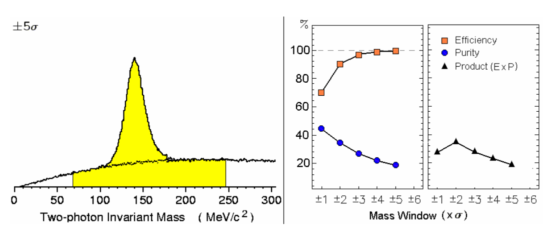

$\pm 6\sigma$

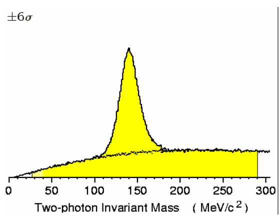

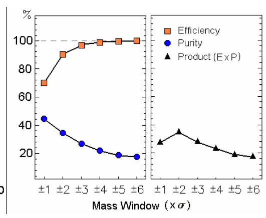

π^0 Estimators

An estimator, based on kinematics of π^0, can be used to discriminate signal and background. Following distributions define our estimators:

- chi-square (χ^2) values from mass constraint
- photon pair opening angles, θ_{12}
- 2D scatter distribution of χ^2 vs θ_{12}

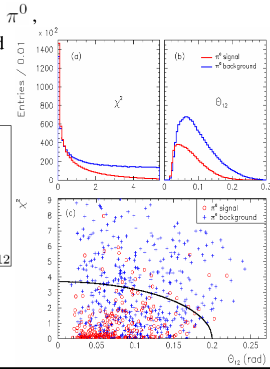

Solid curve has the form:

$$(\frac{\chi^2}{A})^2 + (\frac{\theta_{12}}{B})^2 = 1$$

Ranking Method

After the initial mass window selection, additional improvement can be achived by applying the estimator indirectly with a 'Ranking' method.

The algorithm is as follows:

1. Pion estimator values are calculated for each pion in an **event**
2. Pions candidates are ranked according to **their estimator values**
3. A scan is then made through the list for pairs of pions which share photons. When such a pair exist, **one or both candidates must be false**; the candidate with largest estimator value is removed

Example of applying Ranking method:

SELECTED CANDIDATES *BEFORE RANKING*

#	Pion est.	Photon 1	Photon 2	Truth info.
A	0.05	A1	A2	TRUE
B	0.12	B1	B2	TRUE
X	0.19	D1	E1	FALSE
C	0.28	C1	C2	TRUE
Y	0.45	A1	B2	FALSE
D	0.63	D1	D2	TRUE
Z	0.87	C2	E2	FALSE

SELECTED CANDIDATES *AFTER RANKING*

#	Pion est.	Photon 1	Photon 2	Truth info.
A	0.05	A1	A2	TRUE
B	0.12	B1	B2	TRUE
X	0.19	D1	E1	FALSE
C	0.28	C1	C2	TRUE

To investigate performance of the Ranking method, the **mass window**, and **pion energy** is varied.
The results are compared with the standard method.
Performance is measured in terms of the product: $\varepsilon \times \mathcal{P}$

Performance of the Ranking Method

Mass window

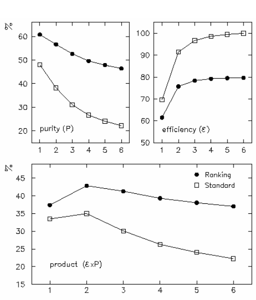

Energy

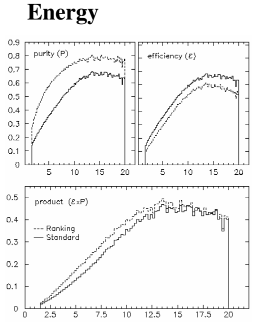

Example Applications

$X \to \pi^+\pi^-\pi^0$

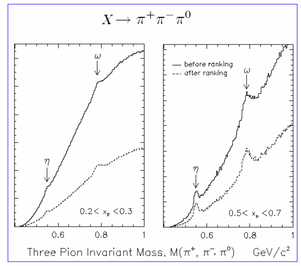

$X \to \pi^0\pi^\pm$

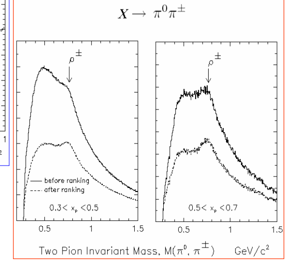

Extraction of the $\rho^{\pm}(770)$ Signal

The rate and cross section of the $\rho^{\pm}$ meson are extracted from the invariant mass distribution of its daughter pions,

$$\rho^{\pm} \to \pi^{0} + \pi^{\pm} \quad (BR \approx 100\%)$$

by fitting the invariant mass to a sum of signal and background functions.

Extraction of $\rho^{\pm}$ yield is complicated by:

- the large with resonance
- the reflection of other mesons (especially $\omega \to \pi^{0}\pi^{+}\pi^{-}$)
- the partially reconstructed signal
- the large combinatorial background
- the residual Bose-Einstein correlations that affects both signal and background shape

Two-pion Invaiant Mass

Charged and Neutral pions are selected as described in Chapter 6.
Invariant mass of two pions is defined as:

$$\begin{aligned} m^{2}(\pi^{\pm},\pi^{0}) &= E^{2}_{\rho^{\pm}} - p^{2}_{\rho^{\pm}} \\ &= (E_{\pi^{\pm}} + E_{\pi^{0}})^{2} - (\vec{p}_{\pi^{\pm}} + \vec{p}_{\pi^{0}})^{2} \end{aligned}$$

where

$$E^{2}_{\pi} = p^{2}_{\pi} + m^{2}_{\pi}$$

with

$$m_{\pi^{\pm}} \approx 140\,\mathrm{MeV/c^{2}}$$

$$m_{\pi^{0}} \approx 135\,\mathrm{MeV/c^{2}}$$

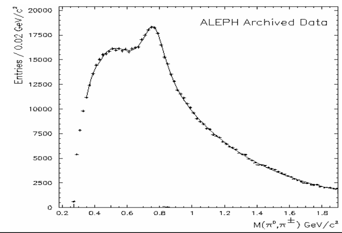

Signal Reconstruction

The data is analysed in

- six intervals of scaled momentum: $x_{p} = p_{\rho}/p_{beam}$
- nine intervals of scaled energy: $x_{E} = E_{\rho}/E_{beam}$

Here $p_{beam} \approx E_{beam}$ (about 45.6 GeV) is the LEP momentum.

Interval	x_p range	x_E range
1	$0.05 \le x_p < 0.10$	$0.050 \le x_E < 0.100$
2	$0.10 \le x_p < 0.20$	$0.100 \le x_E < 0.125$
3	$0.20 \le x_p < 0.30$	$0.125 \le x_E < 0.150$
4	$0.30 \le x_p < 0.40$	$0.150 \le x_E < 0.200$
5	$0.40 \le x_p < 0.50$	$0.200 \le x_E < 0.300$
6	$0.50 \le x_p < 1.00$	$0.300 \le x_E < 0.400$
7		$0.400 \le x_E < 0.600$
8		$0.600 \le x_E < 0.800$
9		$0.800 \le x_E < 1.000$

Note

The results of the measurements

- in x_p intervals are compared with those of ALEPH ρ^0 measurement
- in x_E intervals are compared with OPAL $\rho^{\pm}$ measurement

Using Monte Carlo, we can study the theoretical shape of the momentum and energy distributions for the generated and reconstructed $\rho^{\pm}$ mesons.

The mean efficiency in each interval is used to correct the extracted signal in both Monte Carlo and real data.

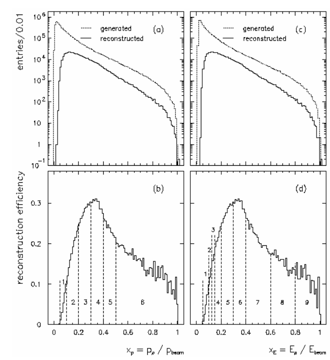

Signal Extraction and Fitting Procedure

Signal Shape

Basic line shape for the $\rho^{\pm}$ signal is a relativistic p-wave BreitWigner:

$$RBW(m) = \frac{m \cdot m_0 \cdot \Gamma(m)}{(m^2 - m_0^2)^2 + m_0^2 \cdot \Gamma^2(m)}$$

with

$$\Gamma(m) = \Gamma_0 \cdot \left(\frac{q}{q_0}\right)^3 \frac{2q_0^2}{q_0^2 + q^2}$$

Monte Carlo (JETSET) uses a non-relativistic Breit-Wigner:

(truncated between 0.3 and 1.3 GeV/c²)

$$BW(m) = \frac{(\Gamma_0/2)^2}{(m - m_0)^2 + (\Gamma_0/2)^2}$$

m is the two-pion invariant mass
m_0 is the resonance peak mass
Γ is the mass dependent width
Γ_0 is the nominal width (FWHM)
q is the momentum of the decay products in the rest frame of parent
q_0 is the momentum when $m = m_0$

Signal Shape

Nominal values are:

$$m_0 = 775.8 \pm 0.5 \ \mathrm{MeV/c^2}$$

$$\Gamma_0 = 151.5 \pm 1.2 \ \mathrm{MeV/c^2}$$

[PDG 2006]

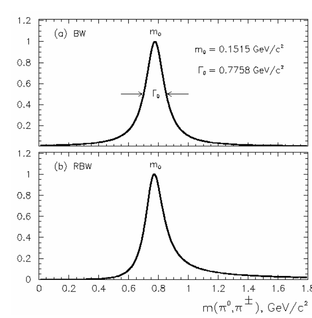

Partially Reconstructed Signal

An important consideration is the effect of partially reconstructed $\rho^{\pm}$ mesons where a π^0 is reconstructed from originating from $\rho^{\pm}$ signal and one that is not.

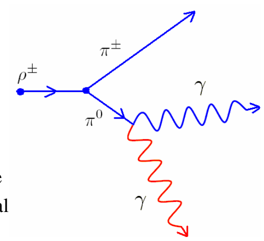

Such a combination contains most of the kinematics of the $\rho^{\pm}$ signal for this reason partial signal has similar, but wider shape.

The width (Γ_0) and peak mass (m_0) are different from the nominal values due to resolution effects, which is dominated by π^0component. The mass resolution (Γ_{res}) and peak mass (m_{res}) of the $\rho^{\pm}$ meson are determined from the Monte Carlo.

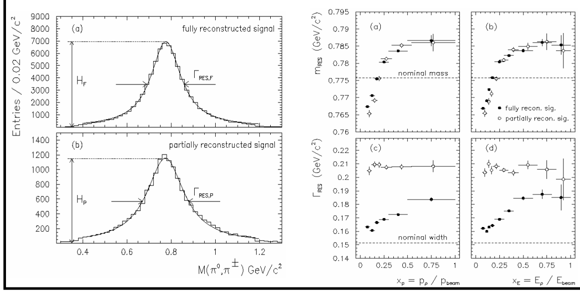

Summary for the Signal function:

- In the fits, nominal values (Γ_0, m_0) are replaced by Γ_{res} and m_{res}
- The height of the partially reconstructed signal (H_P) is parameterised as a function of fully reconstructed signal height (H_F), since they are correlated. The ratio $r = H_F / H_P$ is taken from the Monte Carlo predictions.
- Signal function is parametrised as a sum of two RBW functions:

$$f_s(m) = p_0[RBW_{\mathrm{F}}(m) + RBW_{\mathrm{P}}(m)/r]$$

p_0 is the normalisation constant.

Note that RBW is replaced by BW in the Monte Carlo fits.

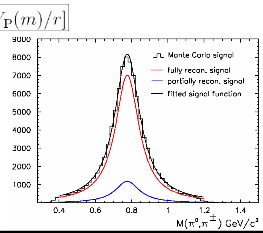

Combinatorial Background

The combinatorial background is parameterised by a smooth function:

$$f_b(m) = p_1 m_t^{p_2} \times \exp(p_3 m_t + p_4 m_t^2 + p_5 m_t^3)$$

where $\quad m_t = m - m_{\pi^0} - m_{\pi^{\pm}}$

The free parameters $p_1 - p_5$ are adjusted by the fitting procedure.

Reflections

$\pi^0\pi^{\pm}$ mass spectra contain reflections from the decays:

$$\omega(782) \rightarrow \pi^0\pi^+\pi^-$$
$$\eta(548) \rightarrow \pi^0\pi^+\pi^-$$
$$K^{*\pm}(892) \rightarrow \pi^0 K^{\pm}$$

Appropriate functions representing each reflection are selected and fitted to the Monte Carlo.

in the Monte Carlo, the height of each reflection is fixed

in real data, *the height of each reflection (taken from MC) is* ***scaled*** *by a value obtained from the real data measurements.*

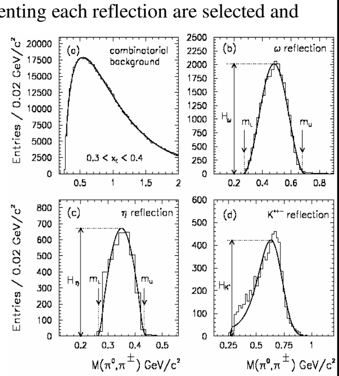

Bose-Einstein Correlations

Bose-Einstein Correlations (BECs) are an apparent attraction in phase-space between identical bosons.

Features of BEC:

- BEC is relevant if and only if identical bosons (such as pions) are close to each other in phase-space.
- Most of the particles generated in hadronic events are pion triplets obeying Bose statistics. As a result, BECs affect the dynamics of the pions in the final state.
- BECs are quantum mechanical effect that must appear during the fragmentaion state. Hence, measurement of BECs can help the understanding of QCD studies.
- BECs are not implemented in MC programs effectively.

Residual Bose-Einstein Correlations

Experimental studies reveal that BECs affect the distribution of effective masses of $\pi^{\pm}\pi^{\pm}$ pairs originating from the IP.

The life-time (~10^{-24}s) and therefore decay length (~ 1fm) of the $\rho^{\pm}$ meson is sufficiently short that pions from the decay $\rho^{\pm} \rightarrow \pi^{\pm} + \pi^{0}$ can be considered as coming from the IP.

Hence a 'Residual' BECs must affect on pions of the $\rho^{\pm}$ meson. Most appearent sign of residual BEC is a distortion in the mass spectra.

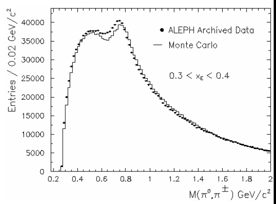

The distortion in real data can be described by interference effect, believed to originate from residual BECs, between the amplitudes of $\rho^{\pm}$ and coherent (non-resonant) background.

A successful parameterisation is performed by Söding Model used before in the ρ^{0} and $\rho^{\pm}$ analysis.

To include the interference effect, the fit function is extended by adding the term:

$$f_i(m) = C\left(\frac{m_{res}^2 - m^2}{m\Gamma(m)}\right) f_s(m)$$

where C is the strength of the interference, and is determined from data fits.

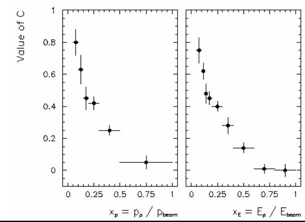

The interference term is a model to describe the distortion affecting both signal and background.

This can be shown by removing the interference term from the real data mass distribution.

C = 0.00 → original distribution
C = 0.30 → close to its fitted value of 0.28

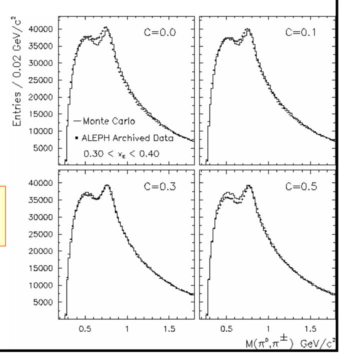

Total Fit Function

Total fit function is built by adding six model functions as follows:

$$F(m) = f_s(m) + f_b(m) + f_i(m) + f_\omega(m) + f_\eta(m) + f_{K^*}(m)$$

Note that $f_i(m)$ is omitted for the Monte Carlo

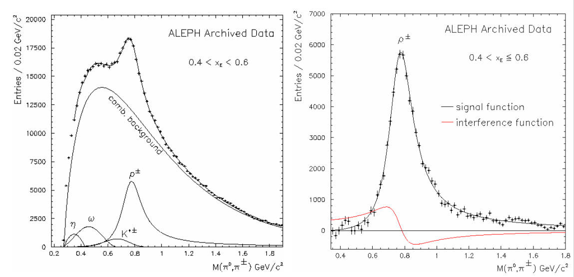

Rates & Cross Sections

Production Rate:

$$R = \frac{S}{N}\frac{1}{\varepsilon}$$

Differential Cross Section:

$$\frac{1}{\sigma_{tot}}\frac{d\sigma}{dx} = \frac{R}{\delta x} = \frac{1}{\delta x}\frac{S}{N}\frac{1}{\varepsilon}$$

N : number of selected hadronic events

S : number of (fitted) signal

δx : width of the energy interval

ε : reconstruction efficiency defined as:

$$\varepsilon = \frac{n_{rec}}{n_{gen}} = \frac{\text{number of reconstructed rho-mesons in MC}}{\text{number of generated rho-mesons in MC}}$$

Systematic Error Analysis

Statistical errors originate from counting (statistical) uncertainties that result in measured values being randomly high or low.

Systematic errors originate from detector effects, uncertainties in models, measurement procedures resulting in measured values being systematically high or low.

Possible source of systematic errors:

- track selection cuts
- fitting procedure
- reflection models
- signal function
- efficiency correction
- uncertainty in the extrapolation to full x_p and x_E ranges

Table 10.4: *Systematic and statistical errors for the $\rho^{\pm}$ rate in each measured momentum interval. All values are expressed in % rounded to one decimal place.*

Source of error		*measured x_p interval*					
	e_{all}	1	2	3	4	5	6
Fit range	1.9	0.4	2.4	2.1	4.4	0.8	6.8
Eff. correction	0.1	0.2	0.2	0.2	0.2	0.2	0.4
Signal width	1.6	3.6	3.2	2.1	2.8	3.5	5.6
Partial signal	*3.0	2.7	3.4	3.5	3.3	3.0	2.1
ω rate	*1.5	2.0	1.7	1.5	0.7	0.3	0.8
η rate	*0.3	0.0	0.0	0.5	1.1	0.2	0.0
$K^{*\pm}$ rate	*0.7	0.0	1.2	2.7	0.1	0.1	2.8
π^0 matching	*0.7	0.6	0.7	0.8	0.7	0.9	0.6
E_γ	2.6	6.0	6.1	3.1	3.2	3.2	3.0
E_{π^0}	1.5	3.5	3.7	2.4	1.5	1.6	4.6
π^0 mass window	1.3	2.6	3.1	2.7	3.5	2.3	3.3
$\chi(dE/dx)$	1.1	2.8	1.3	1.7	0.7	1.6	2.6
d_0	2.0	5.2	1.9	2.7	0.8	0.4	3.7
Systematic error							
(e_{tot})	5.7	10.7	10.0	8.0	8.1	6.5	12.3
Statistical error	1.1	2.5	2.2	1.6	0.9	0.9	2.2
Total error	5.8	11.0	10.2	8.1	8.1	6.6	12.5

Table 10.5: *Systematic and statistical errors for the $\rho^{\pm}$ rate in each measured energy interval. All values are expressed in % rounded to one decimal place.*

Source of Error		*measured x_E interval*								
	e_{all}	1	2	3	4	5	6	7	8	9
Fit range	1.9	4.7	2.6	3.9	3.3	1.5	2.2	3.7	2.8	2.5
Eff. correction	0.1	0.2	0.2	0.2	0.2	0.2	0.2	0.3	0.6	1.8
Signal width	1.6	3.4	3.9	3.8	3.4	3.5	3.3	3.4	3.6	2.8
Partial signal	*3.2	2.9	3.6	3.5	3.7	3.4	3.0	2.7	1.3	1.9
ω rate	*1.7	1.6	2.9	3.2	1.0	2.2	0.3	0.4	0.2	0.1
η rate	*1.5	1.7	2.3	2.5	2.2	0.3	0.2	0.2	1.2	0.0
$K^{*\pm}$ rate	*0.5	0.0	2.7	1.6	0.3	0.1	0.1	0.3	1.9	2.6
π^0 matching	*0.7	0.6	0.7	0.7	0.8	0.7	0.8	0.8	0.6	0.5
E_γ	2.8	6.3	5.0	4.0	4.5	6.4	3.8	4.3	2.5	4.4
E_{π^0}	1.2	3.0	2.4	3.5	0.7	0.4	1.0	3.1	0.2	8.8
π^0 mass window	2.0	4.7	4.7	4.3	3.8	2.8	2.2	3.0	2.2	5.9
$\chi(dE/dx)$	1.1	2.3	4.9	2.5	1.7	0.6	2.1	1.0	4.1	5.7
d_0	0.8	1.7	4.0	2.5	0.7	0.4	0.2	0.4	1.1	3.2
Systematic error										
(e_{tot})	6.1	11.3	12.3	11.0	9.0	9.0	7.1	8.5	7.6	14.2
Statistical error	1.0	2.3	2.7	2.4	1.2	0.9	1.2	1.2	3.4	6.3
Total error	6.2	11.5	12.6	11.3	9.1	9.1	7.2	8.6	8.3	15.5

Results

Table 11.1: *Measured multiplicies and differential cross-sections for the $\rho^{\pm}$ in x_p intervals. The result of summing over the measured x_p intervals is also given, including extrapolation to full x_p range with an additional error due to the uncertainty in the extrapolation.*

x_p range	*Multiplicity $\rho^{\pm}(770)/$ Z decay*	$1/\sigma_{had} d\sigma/dx_p$
0.05-0.10	$0.5622 \pm 0.0142 \pm 0.0603$	$11.2434 \pm 0.2840 \pm 1.2069$
0.10-0.15	$0.3162 \pm 0.0068 \pm 0.0315$	$6.3246 \pm 0.1364 \pm 0.6299$
0.15-0.20	$0.2338 \pm 0.0037 \pm 0.0187$	$4.6756 \pm 0.0736 \pm 0.3731$
0.20-0.30	$0.2335 \pm 0.0022 \pm 0.0189$	$2.3347 \pm 0.0216 \pm 0.1889$
0.30-0.50	$0.1663 \pm 0.0015 \pm 0.0109$	$0.8316 \pm 0.0073 \pm 0.0545$
0.50-1.00	$0.0412 \pm 0.0009 \pm 0.0051$	$0.0823 \pm 0.0018 \pm 0.0102$
0.05-1.00	$1.5532 \pm 0.0164 \pm 0.0880$	
all x_p	$2.5872 \pm 0.0273 \pm 0.1466 \pm 0.0428$	

Table 11.2: *Measured multiplicies and differential cross-sections for the $\rho^{\pm}$ in x_E intervals. The result of summing over the measured x_E intervals is also given, including extrapolation to full x_E range with an additional error due to the uncertainty in the extrapolation.*

x_E range	*Multiplicity $\rho^{\pm}(770)/$ Z decay*	$1/\sigma_{had} d\sigma/dx_E$
0.050-0.100	$0.6050 \pm 0.0137 \pm 0.0683$	$12.0992 \pm 0.2740 \pm 1.3650$
0.100-0.125	$0.1679 \pm 0.0046 \pm 0.0206$	$6.7153 \pm 0.1840 \pm 0.8237$
0.125-0.150	$0.1450 \pm 0.0035 \pm 0.0160$	$5.7990 \pm 0.1400 \pm 0.6407$
0.150-0.200	$0.2258 \pm 0.0027 \pm 0.0204$	$4.5151 \pm 0.1090 \pm 0.4072$
0.200-0.300	$0.2506 \pm 0.0023 \pm 0.0226$	$2.5056 \pm 0.0230 \pm 0.2259$
0.300-0.400	$0.1151 \pm 0.0014 \pm 0.0082$	$1.1511 \pm 0.0140 \pm 0.0820$
0.400-0.600	$0.0820 \pm 0.0010 \pm 0.0070$	$0.4102 \pm 0.0050 \pm 0.0349$
0.600-0.800	$0.0146 \pm 0.0005 \pm 0.0011$	$0.0729 \pm 0.0025 \pm 0.0055$
0.800-1.000	$0.0016 \pm 0.0001 \pm 0.0002$	$0.0078 \pm 0.0005 \pm 0.0011$
0.050-1.000	$1.6076 \pm 0.0154 \pm 0.0981$	
all x_E	$2.5878 \pm 0.0248 \pm 0.1579 \pm 0.0408$	

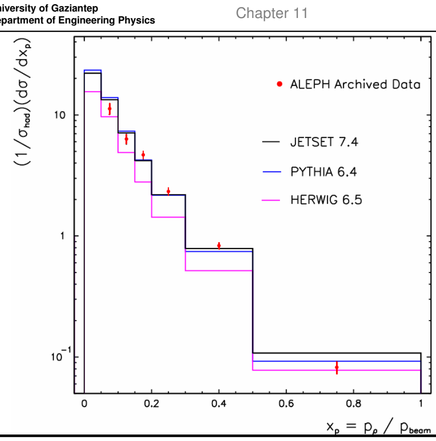

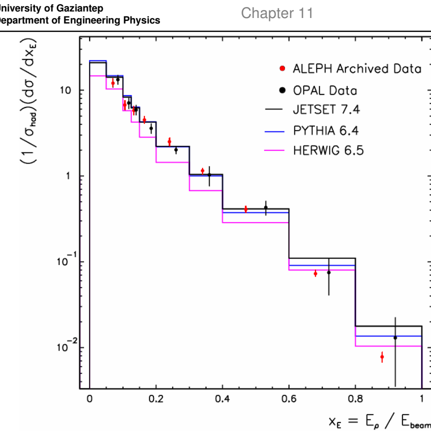

Table 11.3: *Comparison of the total multiplicity of the $\rho^{\pm}$, $N(\rho^{\pm})$ and the ratio $2N(\rho^0)/N(\rho^{\pm})$ as measured by ALEPH to OPAL and Monte Carlo predictions.*

Data set	$N(\rho^{\pm})$	$2N(\rho^0)/N(\rho^{\pm})$
ALEPH data	$2.59 \pm 0.03 \pm 0.15$	$1.12 \pm 0.05 \pm 0.17$
OPAL data	$2.40 \pm 0.06 \pm 0.43$	$1.08 \pm 0.04 \pm 0.20$
JETSET 7.4	2.77	1.06
PYTHIA 6.4	2.85	1.07
HERWIG 6.5	1.93	1.04

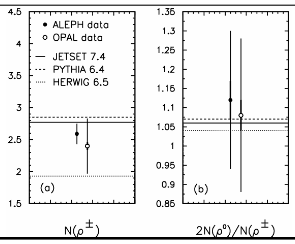

Summary of the Analysis

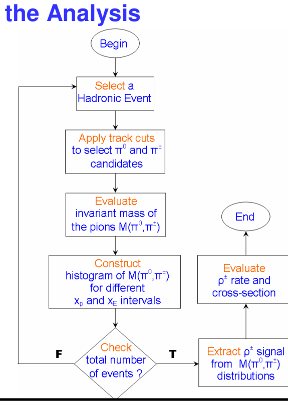

Conclusion

- Inclusive production of the $\rho^{\pm}$ mesons in hadronic Z decays has been observed with the ALEPH detector.
- Measured rate and differential cross-section are in good agreement with OPAL measurements within the error bars.
- Monte Carlo rates obtained from **JETSET** and **PYTHIA** are consistent with the real data measurements of two independent experiments.
- The model for BEC used in our study is same as the OPAL. This model successfully describes distortion in two-pion invariant mass.

Future Work

Experiences gained in this study can be applied to future work in a number of possible areas:

- Particle production involving π^0 decay products
- A measurement of $a_0^{\pm}(980) \rightarrow \eta\pi^{\pm}$
- Much work needs to be done to implement BECs in the MC models, since BECs are not implemented in MC correctly. This is important for LEP and LHC.
- Work on the ATLAS Experiment.

Publications

- A. Beddall, A. Beddall, A. Bingül, Y. Durmaz
A Comparison of Multi-Variate PDE Methods in Neutral Pion Discrimination, Acta Physica Polonica B, 38 187-195 (2007).
- A. Beddall, A. Beddall, A. Bingül, Y. Durmaz
Smoothed multi-variate histogrammed PDEs, and chi^2 optimisation, Computer Physics Communications, 175 700-707 (2006).
- A. Beddall, A. Beddall, A. Bingül
Reducing systematic errors in the selection of signals from two-photon mass spectra, Nuclear Inst. and Methods in Phy. Res A, 554 469-473 (2005).
- A. Beddall, A. Beddall, A. Bingül
A Ranking Method for Neural Pion Selection in High Multiplicity Hadronic Events, Nuclear Inst. and Methods in Phy. Res A 482, 520-527 (2002).

* A Ranking Method for Neutral Pion and Eta Selection in Hadronic Events, TFD 22 (2004)
* Inclusive Production of rho+- mesons in Hadronic Z Decays, AIP 899 (2007)

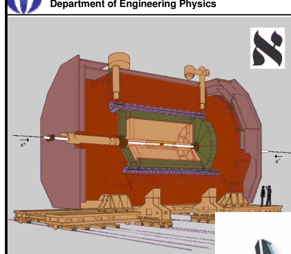

QUESTIONS

?